Anal Bioanal Chem (2011) 401:1331–1339
DOI 10.1007/s00216-011-5202-1

ORIGINAL PAPER

Secretome of the preimplantation human embryo by bottom-up label-free proteomics

Sylvia S. Cortezzi · Jerusa S. Garcia · Christina R. Ferreira · Daniela P. A. F. Braga · Rita C. S. Figueira · Assumpto Iaconelli Jr · Gustavo H. M. F. Souza · Edson Borges Jr · Marcos N. Eberlin

Received: 11 April 2011 / Revised: 23 May 2011 / Accepted: 15 June 2011 / Published online: 8 July 2011

Abstract A bottom-up label-free mass spectrometric proteomic strategy was used to analyse the protein profiles of the human embryonic secretome. Culture media samples used for embryonic culture of patients undergoing intracytoplasmic sperm injection cycles were selected as a test case for this exploratory proof-of-principle study. The media were stored after embryo transfer and then pooled into positive (n=8) and negative (n=8) implantation groups. The absolute quantitative bottom-up technique employed a multidimensional protein identification technology based on separation by nano-ultra-high pressure chromatography and identification via tandem nano-electrospray ionization mass spectrometry with data-independent scanning in a hydrid QqTOF mass spectrometer. By applying quantitative bottom-up proteomics, unique proteins were found exclusively in both the positive- and negative-implantation groups, which suggest that competent embryos express and secrete unique biomarker proteins into the surrounding culture medium. The selective monitoring of these possible secretome biomarkers could make viable procedures using single-embryo transfer.

Keywords Bioanalytical methods · Mass spectrometry · Proteomics · Label-free quantitation · In vitro fertilization · Embryo secretome

S. S. Cortezzi · D. P. A. F. Braga · E. Borges Jr
Sapientiae Institute-Educational and Research Center in Assisted Reproduction,
São Paulo, SP, Brazil 04503-040

J. S. Garcia
Institute of Exact Sciences, Alfenas Federal University,
Alfenas, MG, Brazil 37170-000

C. R. Ferreira · M. N. Eberlin (✉)
ThoMSon Mass Spectrometry Laboratory-Institute of Chemistry,
University of Campinas-UNICAMP,
Campinas, SP, Brazil 13083-970
e-mail: eberlin@iqm.unicamp.br

D. P. A. F. Braga · R. C. S. Figueira · A. Iaconelli Jr · E. Borges Jr
Fertility-Assisted Fertilization Center,
São Paulo, SP, Brazil 01401-002

G. H. M. F. Souza
Mass Spectrometry Applications Research and Development Laboratory, Waters Corporation,
Barueri, SP, Brazil 06455-020

Introduction

In vitro fertilization has been the focus of this year's Nobel Prize in Medicine and intracytoplasmic sperm injection (ICSI) has long been a popular infertility therapy [1]. Despite many instances of improving human fertility and technical progress made in both the clinical and embryological aspects of assisted reproductive technologies (ART), multiple embryo transfer is required to achieve appreciable pregnancy rates [2].

Morphological criteria of embryo development potential seem to have reached a plateau in terms of its ability to assess embryonic potential. In the post-genomic era, many omics efforts have increased our understanding of the relationships between the genome, DNA transcripts, proteins, metabolites, and phenotypes in cells and organisms [3].

Non-invasive approaches for embryonic development potential have the advantages of increasing the knowledge of embryo physiology, therefore allowing the development of methods to predict developmental competence and viability [4]. These approaches include the monitoring of small molecules such as glucose, lactate, pyruvate, or amino acids in the embryo culture media, as well as oxygen consumption. Most recently, the embryonic metabolome [5, 6] and secretome have emerged.

Mass spectrometry (MS) has been shown to be a promising technique to study the embryo secretome. Recently, matrix-assisted laser-desorption ionization–time-of-flight mass spectrometry and surface-enhanced laser-desorption ionization–time-of-flight mass spectrometry have been used to detect differential proteins in human and murine embryo secretome by their molecular masses, but provided no amounts of protein or their identification [7, 8]. Liquid chromatography–electrospray ionization mass spectrometry of tryptic digests of control and conditioned murine media was able to characterise peptides indicative of 16 proteins [8].

The standard MS proteomics approach involves pre-separation of intact proteins via two-dimensional gel electrophoresis or chromatography techniques with fraction collectors, which requires extensive sample manipulation [9, 10]. In embryology, the small samples normally available and the large amount of proteins within these protein pools has led to poor sensitivity, particularly for the less-abundant proteins. Most of embryology proteomics has, therefore, focused on distinguishing and localizing target proteins, which has limited the understanding of embryologic physiology [9, 11].

Advances in MS proteomic technologies, especially involving nano-ultra-high pressure chromatography (nano-UPLC) and label-free quantification with mass spectrometry with data-independent scanning (MS^E) mode, have allowed the use of minimal amounts of sample and the efficient identification of an increased number of proteins [12, 13]. The utilized data-independent nano-UPLC-MS^E method means that a parallel acquisition approach for each peptide and corresponding fragments can be used, resulting in improved MS duty cycles. Unlike traditional MS/MS data-dependent acquisition (DDA) approaches, MS^E requires no real-time decisions on the selection of precursor ions, such as MS/MS switching thresholds or the recognition and subsequent selection of specific charge states for fragmentation. As a consequence, partial sampling of chromatographic peaks is avoided, which eliminates some of the drawbacks associated with current data-directed nanoLC-MS/MS approaches [14].

In this study, we have tested whether the label-free bottom-up MS^E proteomic technique would serve to characterise the protein profiles of the human embryonic secretome. As a test case, embryos of patients undergoing ICSI cycles were selected.

Materials and methods

Patients

Pooled culture medium samples from 16 embryos obtained from eight patients undergoing oocyte retrieval for ICSI were used. Causes of infertility were defined within the following categories: male factor (62.5%), ovarian factor (25%), and endometriosis (12.5%). The samples were pooled according to the embryo implantation outcomes: eight embryos were retrieved from four patients with positive pregnancy results and 100% successful implantation (positive-implantation group) and eight embryos were retrieved from four patients showing negative outcomes with 0% implantation (negative-implantation group). Written informed consent was obtained, in which patients agreed to share the outcomes of their cycles for research purposes.

Controlled ovarian stimulation

Controlled ovarian stimulation was achieved by long-term pituitary downregulation using a gonadotropin-releasing hormone antagonist (Cetrotide®, Serono, Geneva, Switzerland) followed by ovarian stimulation with recombinant-FSH (Gonal-F®, Serono, Geneva, Switzerland). Oocyte retrieval was performed 35 h after the administration of recombinant human chorionic gonadotrophin (rhCG, Ovidrel™, Serono, Geneva, Switzerland) through transvaginal ultrasonography.

Preparation of oocytes

After retrieval, oocytes were incubated in culture medium (G-1™-V1, Vitrolife, Kungsbacka, Sweden), covered with mineral oil (Ovoil™, Vitrolife, Kungsbacka, Sweden) and incubated 37 °C and 6% CO_2 for 5 h. Cumulus cells were removed with a 30-s exposure to HEPES-buffered medium containing 80 IU mL^{-1} hyaluronidase (Irvine Scientific, Santa Ana, USA), after which the coronal cells were manually removed using a finely drawn glass Pasteur pipette (Humagen Fertility Diagnostics, Charlottesville, Virginia, USA). The denuded oocytes were then assessed for nuclear status. Oocytes that were observed to have released the first polar body were considered mature and used for ICSI.

Intracytoplasmic sperm injection

For ICSI, oocytes were individually placed in 4-μL droplets of buffered medium (G-Mops™-V1, Vitrolife, Kungsbacka,

Sweden). Sperm were placed in a central 4-μL droplets of polyvinylpyrrolidone solution (Irvine Scientific, Santa Ana, USA) in a 50×40-mm glass culture dish (WillCo-dish®, New Jersey, USA) covered with warm mineral oil (Ovoil™, Vitrolife, Kungsbacka, Sweden).

Assessment of fertilization, embryo quality, and embryo transfer

Embryos were kept in a 50-μL drops of G1 medium (VitroLife, Kungsbacka, Sweden) supplemented with 10% HSA covered with mineral oil in a humidified atmosphere with 5% CO_2 at 37 °C until transfer.

Fertilization assessment was performed 18 h after ICSI, after which the culture medium was refreshed and the embryos were further cultured for 48 h. Embryo quality was evaluated under an inverted microscope. The following parameters were recorded: (1) the number of blastomeres, (2) the fragmentation percentage, (3) variation in blastomere symmetry, (4) the presence of multinucleation, and (5) defects in the zona pellucida and the cytoplasm. Top-quality embryos were defined as those having all of the following characteristics: six to ten cells on the third day of development, less than 15% fragmentation, symmetric blastomeres, absence of multinucleation, colourless cytoplasm with moderate granulation and no inclusions, absence of perivitelline space granularity, and absence of zona pellucida dysmorphism. Embryos lacking any of the above characteristics were considered to be of medium or low quality.

Embryo transfer was performed on the third day of development. One to three embryos from each couple were transferred to the patient. Embryo selection for transfer was performed blindly in the experimental group and was based on embryo morphology.

Following embryo transfer, the remaining culture medium was individually collected and stored at −20 °C. Subsequent to implantation confirmation, culture medium samples from embryos having positive (n=8) and negative (n=8) pregnancy outcomes were pooled.

Sample preparation

Initially, 400 μL of pooled culture medium samples from the control group (culture medium maintained in the incubator) and those from embryos having positive or negative-implantation outcomes were precipitated using a solution containing 10% (m/v) trichloroacetic acid in acetone at −20 °C in a sample: precipitating agent ratio of 1:5. Mixtures were kept in contact overnight, and pellets were centrifuged at 4 °C for 5 min at 13,000×g in an ultracentrifuge (Eppendorf AG, Hamburg, GE). Next, the pellets were dissolved in 1,000 μL of phosphate buffer (pH 7.2). Total protein concentration measurements in the samples were determined according to the Bradford method, employing bovine serum albumin (Sigma Aldrich, St. Louis, MO, USA) as a standard [15]. The measurements were done in triplicate, at 595 nm, using a Micronal B582 spectrophotometer (Micronal, São Paulo, SP, Brazil). Total protein concentration at culture media from positive and negative-implantation groups was respectively 10.96 and 7.66 mg mL^{-1}.

After protein quantification, the appropriate volume of each sample containing 50 μg of protein was submitted to centrifugation at 4°C, 13,000×g in the same equipment previously described using an Amicon Ultra centrifugal filter (Millipore, Billerica, USA) with a cut-off value of 3 kDa to desalt and concentrate the samples until the sample volume was reduced to 50 μL and the final protein concentration was 1 μg μL^{-1}. Finally, a tryptic digestion procedure was initiated by denaturing the protein samples with 0.2% (m/v) *Rapi*Gest™ SF Surfactant (Waters, UK) for 15 min at 80 °C. Next, the proteins were reduced using 10 mM dithiothreitol (prepared fresh in 50 mM NH_4HCO_3) for 30 min at 60 °C. The samples were then cooled to room temperature and alkylated with a solution containing 10 mM iodoacetamide also prepared in 50 mM NH_4HCO_3. The samples were maintained in a dark chamber at 25 °C for 30 min. The sample proteolysis was performed with trypsin at 1:100 (m/m) enzyme/protein ratio at 37 °C in a block heater overnight. Following digestion, 5% (v/v) trifluoroacetic acid was added to the samples at 37 °C for 90 min to hydrolyse the *Rapi*Gest™ SF solution (Waters, Milford, USA). In the last step of the procedure, a MassPREP™ Protein Digestion Standard alcohol dehydrogenase UNIPROT P00330 (Waters, Milford, USA) was added as an internal standard for quantification in a concentration of 25 fmol μL^{-1}.

Nano-UPLC tandem nano-ESI-MS^E conditions

Nano-UPLC with nano-electrospray ionization (nano-ESI) with data-independent scanning (MS^E) experiments were performed using a 90 min reversed phase gradient from 3% to 40% (v/v) of acetonitrile with 0.1% (v/v) formic acid in a nanoACQUITY UltraPerformanceLC® UPLC® chromatography system (Waters, Milford, USA) with a flow rate of 600 ηL min^{-1}. A nanoscale nanoACQUITY UPLC 2D kit columns (Waters, Milford, USA) with BEH130 C_{18} 1.7 μm, 100 μm×100 mm was used in combination with a Strong Cation-Exchange column (SCX) 5 μm, 300 Å, 0.18×23.5 mm Nano-Ease Trap Column (Waters, Milford, USA). Typical on-column sample loads were 750 ng of the total protein digests. For all measurements, a Synapt™ HDMS™ mass spectrometer (Waters, Manchester, UK) was operated in the "W" mode with a typical resolving power 20,000 full width at half maximum (FWMH). All analyses were performed using

positive-ion mode ESI(+) and a NanoLockSpray™ ionization source. The lock mass channel was sampled every 30 s. The mass spectrometer was calibrated with a [Glu1]-Fibrinopeptide B human (GFP) solution (100 fmol μL^{-1}) delivered through the reference sprayer of the NanoLockSpray™ source. The doubly charged peptide ion ($[M+2H]^{2+}$) was used for initial single point calibration, and MS/MS fragment ions of GFP were used to obtain the final instrument calibration. MS^E experiments were automatic and planned to step between standard MS (3 eV) and elevated collision energies MS^E (12–45 eV) applied to the trap "t-wave" CID (collision-induced dissociation) cell with argon gas; the transfer collision cell was adjusted for 1 eV, using a scan time of 0.6 s and automatic interscan, both in low energy and high energy CID and an orthogonal acceleration time of flight (*oa*-TOF). MS^E was acquired over the *m/z* range of 50–1990. The RF offset (MS profile) was adjusted such that the LC/MS^E data were effectively acquired from *m/z* 200 to 1,990, which ensured that any fragment ions of *m/z* values less than *m/z* 200 observed in the LC/MS^E data were known to arise from dissociations in the collision cell.

Database searching

Protein identifications and quantitative data package were generated by dedicated algorithms [16] and protein comparisons with a species-specific database [17]. For proper spectra processing and database search conditions, a ProteinLynxGlobalSERVER™ v.2.4 (PLGS) with an Expression^E informatics v.2.4 license was used. A UniProtKB/Swiss-Prot Release 57.1 and a UniProtKB/TrEMBL Release 40.1 database were also used and the search conditions were based on taxonomy of *Homo sapiens*, one missed cleavage by trypsin, variable modifications by carbamidomethyl, acetyl *N*-term, and oxidation. Proteins identified were organised using PLGS into a list detailing protein unique to each condition and a logarithm ratio between the different groups. Only proteins with attendance scores and confidence intervals higher than 99% according to the dedicated algorithm [18, 19], respectively, were considered acceptable in these database searches, and when the same protein was identified for different fragment ions, those presenting the highest score were considered for further comparisons and data presentation [18, 20].

Results

General characteristics

From eight ICSI cycles, 77 MII oocytes were retrieved. Of these oocytes, 54 (70.1%) had normal fertilization, defined as the presence of two distinct pronuclei, and 16 embryos were transferred. As Table 1 shows, the groups were equal regarding all general cycle characteristics.

Presence of differentially secreted proteins

Figure 1 summarises the embryo secretome analysis workflow used. Eighteen sequences detected exclusively in the control group media samples were excluded from the analysis. Figure 2 shows plots of the average log intensity from peptides selected as $[M+H]^+$ in the *m/z* range of 250 up to 8500 for the positive-implantation group (*x*-axis) and for the negative-implantation group (*y*-axis). When submitted to databank analysis and after data filtering, the clustering tool of the Expression^E informatics, differentially expressed peptides and their corresponding proteins were assigned if their scores and confidence intervals were higher than 99%, respectively.

Identification of differentially secreted proteins

We only considered data regarding unique proteins secreted by embryos in each group, i.e., those absent in the control group corresponding to incubated culture medium. From the 64 initial products observed, 29 were uniquely expressed in the positive (corresponding to 18 protein sequences—Table 2) or negative (corresponding to 11 protein sequences—Table 3) implantation groups. When repeated products corresponding to the same protein were accounted for, a total of 25 proteins were identified, 15 in the positive group and ten in the negative group. Regarding function, 16 proteins are related to binding in general, six proteins have catalytic activity, two act as transcription factors, three proteins have unidentified functions, and the remaining proteins are known to have various functions within the cell. Seven proteins have two gene ontology molecular functions annotated. Figure 3 displays the proteins identified in terms of their functions for both the positive- and negative-implantation groups.

In the positive-implantation group, three sequences (two sequences of 1246 AA and one of 960 AA) were assigned to the same protein, called Jumonji (JARID2), a nuclear protein from a histone methyltransferase complex. In the negative-implantation group, two sequences were assigned to a testis-specific gene 10 (TSGA10) protein, with sequences of 297 AA and 621 AA.

Discussion

This is the first time a quantitative label-free bottom-up approach using 2D nano-UPLC chromatography separation via the nanoUPLC-MS^E technique is used as a strategy to study the human embryo secretome. This proof-of-principle communication is intended to highlight the potential of this

Table 1 Patient characteristics for the positive- and negative-implantation groups

	Positive group	Negative group	*P*
Patients age	35.7±3.3	34.2±5.4	0.662
FSH (IU)	2681±646	2469±361	0.597
Follicles	19.5±13.9	19.3±15.8	0.982
MII oocytes	11.2±6.6	8±5.2	0.475
Fertilization rate (%)	69.7±24.4	71.2±25.2	0.938
High quality embryo rate (%)	79.3±24.9	68.3±47.2	0.702

Values expressed as mean± SEM, unless otherwise noted. Student's *t* test

technology. Although we have used only one experimental replicate of embryos pooled in this exploratory study, to assure proper sensitivity in biomarker screening, we envisage that further improvements in sensitivity and the monitoring of a specific set of a few most important biomarkers will allow for the ultimate goal of secretome monitoring of a single embryo.

The protein pool secreted by the cells at any given time or under specific physiological conditions composes the secretome, which may provide specific embryo biomarkers. The secretome profile is of particular interest in ART due to its non-invasive predictive power for proper embryo development. If secretome biomarkers are identified, and if they can be monitored with enough detectability for a single embryo, single transfer protocols using the most competent embryo would become viable, thus, eliminating the risk and undesirable outcomes of multiple pregnancies [9, 10].

On-line 2D chromatography separation associated with nanoUPLC-MS^E has emerged as a new frontier in proteomics. This approach allows the quantitative analysis of highly complex protein mixtures with protein identification in a label-free approach based on prototypic peptides [21, 22]. The 2D chromatography eliminates the need for 2D gels, and the whole "system sample" is digested into peptides (bottom-up proteomics). The complex peptide mixture is then submitted to nano-UPLC coupled to a nano-ESI source and further data-independent scanning through MS^E is used to improve sensitivity and dynamic range [3, 22, 23]. Owing to the superior dynamic range and selectivity, techniques for depletion of albumin and other

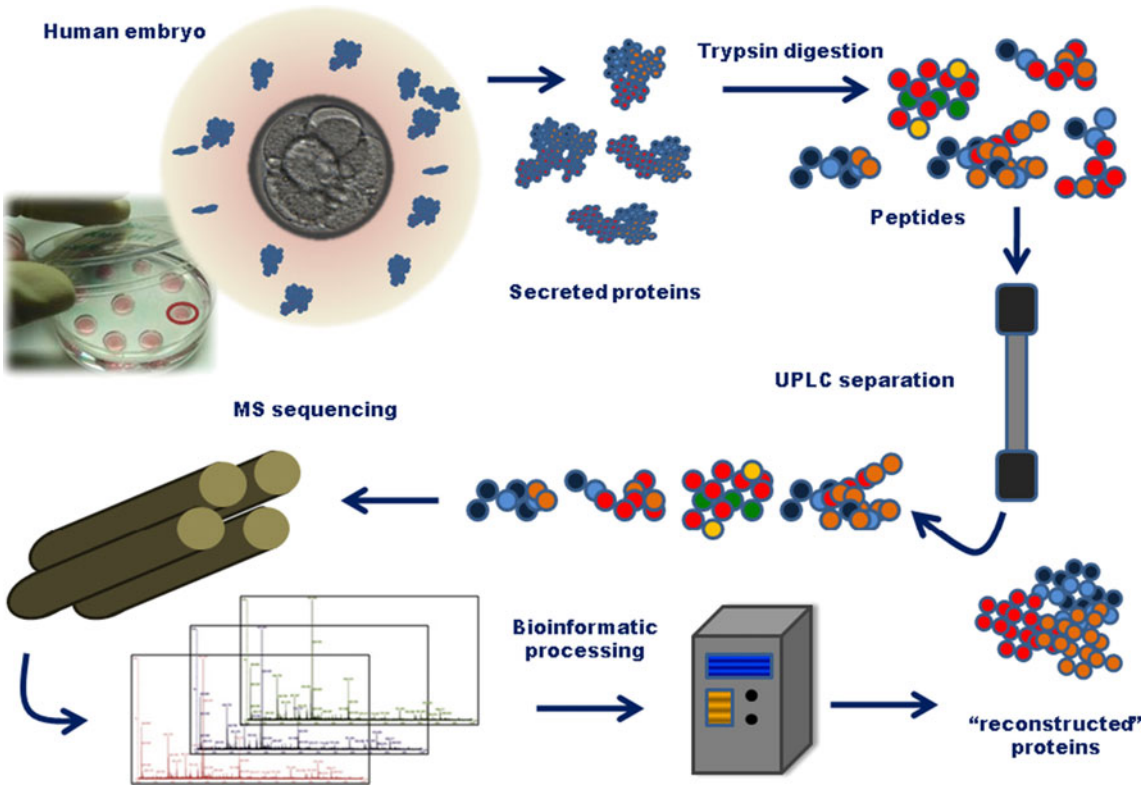

Fig. 1 Workflow of bottom-up proteomic analysis of the human embryos secretome. Precipitated proteins in the culture media are digested by trypsin, and the resulting peptides are separated by nano-UPLC and characterised by nano-ESI-MS^E, through their masses and fragmentation profiles. Using databank search and bioinformatic tools, proteins are identified by the matching of their constituent peptides

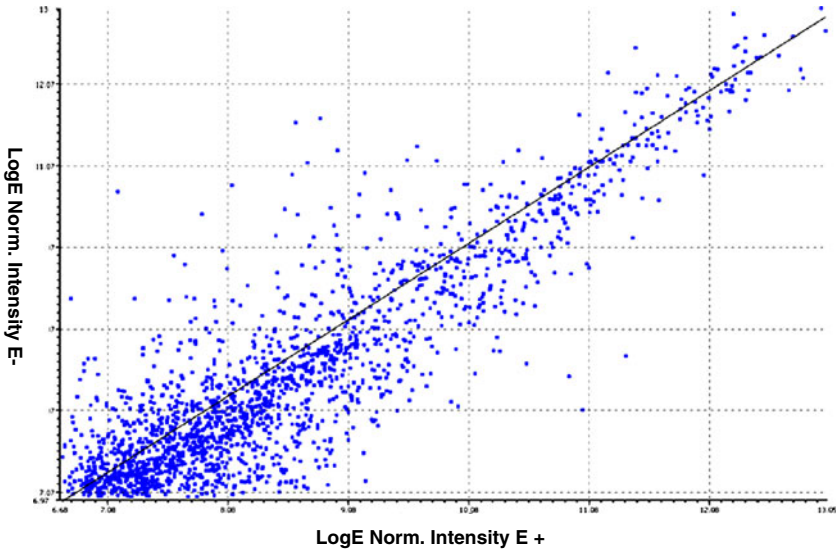

Fig. 2 Sloping plot of normalized log intensity. Association of clustered exact-mass retention time (EMRTs) among samples E− with E+(log-normalized intensity). For each corresponding EMRT component, the average log intensity from each condition is plotted along each of the two axes. The ability to display these conditional profiles for all matched EMRTs enables comprehensive global comparisons rather than multiple binary comparisons. Using this approach, the EMRTs can be fast screened and characterised on the basis of their collective behaviour across the multiple conditions. The data are presented as obtained from the clustered dataset from the clustering tool of the Expression^{E} Informatics software

abundant proteins are also not required, which helps to decrease analytical inconsistency. Hybrid mass spectrometers, such as the Q-TOFs, are generally used for high resolution and high-accuracy spectra both for precursor and fragment ions and improved identification particularly of minor proteins, especially when associated with ion-mobility separations for increased dynamic range [23].

The nanoUPLC-MS^{E} method used in this study acquires precursor and product ion data on all charge states of an eluting peptide across its entire chromatographic peak width, providing more comprehensive precursor and product ion spectra. This strategy favours the identification of a greater number of peptides and proteins [18] with improved sequence coverage and statistical rigour when compared with conventional LC-MS/MS methods [18, 22].

The nanoUPLC-MS^{E} technology has already been applied to study the embryo secretome and a single protein biomarker has been found to correlate with human implantation outcome. The MW of the corresponding proteins have been reported for spent media of human embryos from controls and patients with polycystic ovaries [7, 11]. The protein-array technology was also employed to analyze the secretome profile of human blastocysts that successfully implanted to reveal some possible biomarkers in human [24] and some proteins of murine embryos secretome were reported [8]. However, these studies with human spent media were not aimed at characterising the embryo secretome profile before and around the embryonic genome activation (EGA), given that they refer to the blastocyst stage. We have shown that nanoUPLC-MS^{E} using minimal amounts of samples is able to identify unique proteins expressed exclusively in association with different implantation outcomes during EGA, although the maternal or zygotic sources of these proteins are still to be determined. These proteins are likely to be mostly maternal, since early embryonic development is first dependent on maternally stored transcripts, which are gradually depleted until the embryo produces its own transcripts after a switch to the embryonic expression programme [25–27].

These protein profile differences between the implantation groups may result from few numbers of samples, but the data seem to support that indeed competent embryos display unique protein expression. This is a feature that has also been observed in another study comparing the protein profiles in the spent culture media of implanted versus non-implanted blastocysts by protein microarrays. In that study, it was reported as differential profiles between the groups, with a decrease in GM-CSF and CXCL13 in the implanted blastocyst group [24]. Human and mouse embryonic secretome analyses have revealed distinct protein profiles at different developmental stage. Ubiquitin has been proposed as a biomarker due to its correlation with ongoing blastocyst development [9].

In the positive-implantation group, three sequences (two sequences of 1246 AA and one of 960 AA) were assigned to the same protein, called Jumonji (JARID2). This protein composes a histone methyltransferase complex called Polycomb Repressive Complex 2 (PRC2). This complex modifies chromatin methylation to silence many embryonic patterning genes, acting as a negative regulator of cell

Table 2 Proteins secreted in culture media and identified by nano-UPLC coupled to nano-ESI-MS^E for the positive-implantation group

Swiss-Prot ID	Description	Gene name	Protein score	Sequence lenght	Molecular function
A8K9P0	A8K9P0 HUMAN cDNA FLJ78413 highly similar to *Homo sapiens* albumin mRNA OS *H. sapiens* PE 2 SV 1		7,676.02	608 AA	Transport
HPTR_HUMAN	Isoform 2 of haptoglobin-related protein OS *H. sapiens* GN HPR	HPR	467.65	348 AA	Catalytic activity/ Binding
AGRP_HUMAN	Agouti-related protein OS *H. sapiens* GN AGRP PE 1 SV 1	AGRP	278	132 AA	Hormonal activity
Q5QPP3	Q5QPP3 HUMAN UDP galactose 4 epimerase fragment OS *H. sapiens* GN GALE PE 2 SV 1	RP5-886K2.6-007	174.88	227 AA	Binding
B7WNR2	B7WNR2 HUMAN putative uncharacterized protein SDK1 OS *H. sapiens* GN SDK1 PE 4 SV 1	SDK1	77.05	286 AA	Binding
B7WNY2	B7WNY2 HUMAN putative uncharacterized protein SDK1 OS *H. sapiens* GN SDK1 PE 4 SV 1	SDK1	74.58	2193 AA	Binding
CARP_HUMAN	Protein CARP OS *H. sapiens* GN CARP PE 1 SV 1	CARTPT	66.43	328 AA	Binding
CM027_HUMAN	Uncharacterized protein C13orf27 OS *H. sapiens* GN C13orf27 PE 2 SV 1	C13orf27	58.71	227 AA	Unknown function
Q4ZG79	Q4ZG79 HUMAN putative uncharacterized protein KLF7 fragment OS *H. sapiens* GN KLF7 PE 2 SV 1	KLF7	57.5	268 AA	Transcription factor activity/ Binding
B5MD94	B5MD94 HUMAN putative uncharacterized protein QRICH2 OS *H. sapiens* GN QRICH2 PE 4 SV 1	QRICH2	52.42	1429 AA	Binding
B4DS72	B4DS72 HUMAN cDNA FLJ57033 highly similar to antigen peptide transporter 2 OS *H. sapiens* PE 2 SV		49.22	768 AA	Transport
RSRC2_HUMAN	Isoform 2 of arginine serine rich coiled coil protein 2 OS *H. sapiens* GN RSRC2	RSRC2	48.23	434 AA	Unknown function
A8K9Z6	A8K9Z6 HUMAN Jumonji AT rich interactive domain 2 isoform CRA a OS *H. sapiens* GN JARID2 PE 2 SV	JARID2	47.31	1246 AA	Binding
JARD2_HUMAN	Protein Jumonji OS *H. sapiens* GN JARID2 PE 1 SV 2	JARID2	47.31	1246 AA	Binding
SPAG6_HUMAN	Isoform 3 of Sperm associated antigen 6 OS *H. sapiens* GN SPAG6	SPAG6	42.17	509 AA	Binding
PGPS1_HUMAN	Isoform 3 of CDP diacylglycerol glycerol 3 phosphate 3 phosphatidyltransferase mitochondrial OS Ho	PGS1	43.69	556 AA	Binding
B7Z5S5	B7Z5S5 HUMAN cDNA FLJ55641 highly similar to Jumonji protein Jumonji ARID domain containing protein	JARID2	43.16	960 AA	Binding
C7SDG0	C7SDG0 HUMAN brefeldin A-resistant Arf guanine nucleotide exchange factor 1b Fragment OS *H. sapiens*	BRAG1	35.09	257 AA	Catalytic activity

Table 3 Proteins secreted in culture media and identified by nano-ESI-MS^E for the negative-implantation group

Swiss-Prot ID	Description	Gene name	Protein score	Sequence lenght	Molecular function
Q0VAC5	Q0VAC5 HUMAN HP protein OS *Homo sapiens* GN HP PE 2 SV 1	HP	828.13	347 AA	Binding
B7Z925	B7Z925 HUMAN cDNA FLJ55754 highly similar to *H. sapiens* testis-specific 10 TSGA10 mRNA OS Hom	TSGA10	69.42	297 AA	Structural activity
B8ZZZ9	B8ZZZ9 HUMAN Putative uncharacterized protein TSGA10 OS *H. sapiens* GN TSGA10 PE4SV 1	TSGA10	69.18	621 AA	Structural activity
PTPRS_HUMAN	Isoform PTPS F4 7 of receptor-type tyrosine protein phosphatase S OS *H. sapiens* GN PTPRS	PTPRS	52.35	1948 AA	Catalytic activity/ Binding
B3KQ13	B3KQ13 HUMAN cDNA FLJ32614 fis clone STOMA2000121 highly similar to Homo sapiens kynurenine aminot	KAT3	51.02	420 AA	Catalytic activity
B5MD10	B5MD10 HUMAN Putative uncharacterized protein OR10J5 OS *H. sapiens* GN OR10J5 PE 4SV 1	OR10J2P	45.83	309 AA	Receptor activity
B4DXQ7	B4DXQ7 HUMAN cDNA FLJ51378 highly similar to *H sapiens* NYD SP28 protein NYD SP28 mRNA OS *Homo*	NYD-SP28	42.16	341 AA	Unknown function
CLC14_HUMAN	C type lectin domain family 14 member A OS *H. sapiens* GN CLEC14A PE 1 SV 1	CLEC14A	39.94	490 AA	Binding
LHX9_HUMAN	Isoform 4 of LIM homeobox protein Lhx9 OS *H. sapiens* GN LHX9	LHX9	38.95	397 AA	Transcription factor activity/binding
B4DPN0	B4DPN0 HUMAN cDNA FLJ51265 moderately similar to Beta 2 glycoprotein 1 Beta 2 glycoprotein I OSH	APOH	38.86	274 AA	Binding
Q541F1	Q541F1 HUMAN ubiquitin carboxyl terminal hydrolase OS *H. sapiens* GN VDU2 PE 2 SV 1	USP20	28.35	914 AA	Catalytic activity binding

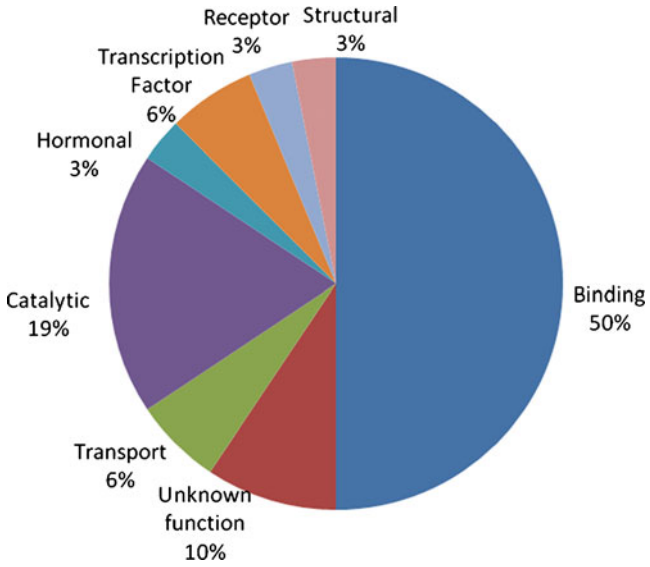

Fig. 3 Protein distribution according to a function that indicates all proteins (n=25) that were expressed exclusively in positive- and negative-implantation groups

proliferation signalling, but may also be related to cell differentiation. PRC2, therefore, restricts gene expression to the appropriate cell populations essential for development, differentiation, and maintenance of cell fates [28–30].

TSGA10 was the most frequent protein detected only in the negative-implantation group. TSGA10 is a perinuclear protein which has structural activity and occurs in actively dividing and foetal differentiating tissues during developmental stages of mouse embryos. This expression pattern suggests that it may be involved in cell differentiation, cell division, and cell migration, therefore enhancing gene expression [31, 32].

Conclusions

Quantitative proteomics via the nanoUPLC-MS^E technique has been shown to provide an effective non-invasive technique able to characterise the protein profiles of human embryonic day-3 secretome, which is the crucial period for the success of ART procedures. It also seems to provide a tool to increase our understanding of early embryonic cellular processes correlated to the embryo genome activation and implantation signalling. The differential protein profiles indicate the existence of potential biomarkers in embryo secretome which is able to provide key information about the embryonic metabolism profile. A pool of embryos was used in this exploratory work to search for possible specific biomarkers but the next step will focus on the use of selective monitoring of a set of these potential biomarkers via multiple reaction monitoring methods to validate their use as diagnostic markers. The improved detectability of such monitoring could demonstrate the viability of this approach to investigate

single-embryo secretome hence allowing the selection of the best sample for single-embryo transfer.

Acknowledgments We thank the Brazilian Science Foundations CNPQ, CAPES, FINEP, and FAPESP for financial assistance.

We thank to Kevin S. Kerian for English language review of this manuscript.

References

1. Palermo G, Joris H, Devroey P, Van Steirteghem AC (1992) Pregnancies after intracytoplasmic injection of single spermatozoon into an oocyte. Lancet 340:17–18
2. Pandian Z, Bhattacharya S, Ozturk O, Serour G, Templeton A (2009) Number of embryos for transfer following in-vitro fertilisation or intra-cytoplasmic sperm injection. Cochrane Database Syst Rev 2: CD003416.
3. Katz-Jaffe MG, McReynolds S, Gardner DK, Schoolcraft WB (2009) The role of proteomics in defining the human embryonic secretome. Mol Hum Reprod 15:271–277
4. Hamel M, Dufort I, Robert C, Gravel C, Leveille MC, Leader A, Sirard MA (2008) Identification of differentially expressed markers in human follicular cells associated with competent oocytes. Hum Reprod 23:1118–1127
5. Bromer JG, Seli E (2008) Assessment of embryo viability in assisted reproductive technology: shortcomings of current approaches and the emerging role of metabolomics. Curr Opin Obstet Gynecol 20:234–241
6. Aydiner F, Yetkin CE, Seli E (2010) Perspectives on emerging biomarkers for non-invasive assessment of embryo viability in assisted reproduction. Curr Mol Med 10:206–215
7. Katz-Jaffe MG, McCallie BR, Janesch A, Filipovits JA, Schoolcraft WB, Gardner DK (2010) Blastocysts from patients with polycystic ovaries exhibit altered transcriptome and secretome. Reprod Biomed Online 21:520–526
8. Beardsley AJ, Li Y, O'Neill C (2010) Characterization of a diverse secretome generated by the mouse preimplantation embryo in vitro. Reprod Biol Endocrinol 8:71
9. Katz-Jaffe MG, Schoolcraft WB, Gardner DK (2006) Analysis of protein expression (secretome) by human and mouse preimplantation embryos. Fertil Steril 86:678–685
10. Katz-Jaffe MG, Gardner DK (2008) Symposium: innovative techniques in human embryo viability assessment. Can proteomics help to shape the future of human assisted conception? Reprod Biomed Online 17:497–501
11. Katz-Jaffe MG, Gardner DK, Schoolcraft WB (2006) Proteomic analysis of individual human embryos to identify novel biomarkers of development and viability. Fertil Steril 85:101–107
12. Chambery A, Colucci-D'Amato L, Vissers JP, Scarpella S, Langridge JI, Parente A (2009) Proteomic profiling of proliferating and differentiated neural mes-c-myc A1 cell line from mouse embryonic mesencephalon by LC-MS. J Proteome Res 8:227–238
13. Levin Y, Wang L, Ingudomnukul E, Schwarz E, Baron-Cohen S, Palotas A, Bahn S (2009) Real-time evaluation of experimental variation in large-scale LC-MS/MS-based quantitative proteomics of complex samples. J Chromatogr B Analyt Technol Biomed Life Sci 877:1299–1305
14. Patel VJ, Thalassinos K, Slade SE, Connolly JB, Crombie A, Murrell JC, Scrivens JH (2009) A comparison of labeling and label-free mass spectrometry-based proteomics approaches. J Proteome Res 8:3752–3759
15. Bradford MM (1976) A rapid and sensitive method for the quantitation of microgram quantities of protein utilizing the principle of protein-dye binding. Anal Biochem 72:248–254
16. Silva JC, Denny R, Dorschel CA, Gorenstein M, Kass IJ, Li GZ, McKenna T, Nold MJ, Richardson K, Young P, Geromanos S (2005) Quantitative proteomic analysis by accurate mass retention time pairs. Anal Chem 77:2187–2200
17. Krämer-Albers E-M, Bretz N, Tenzer S, Winterstein C, Möbius W, Berger H, Nave K-A, Schild H, Trotter J (2007) Oligodendrocytes secrete exosomes containing major myelin and stress-protective proteins: Trophic support for axons? Proteomics Clin. Appl 1:1446–1461
18. Li GZ, Vissers JP, Silva JC, Golick D, Gorenstein MV, Geromanos SJ (2009) Database searching and accounting of multiplexed precursor and product ion spectra from the data independent analysis of simple and complex peptide mixtures. Proteomics 9:1696–1719
19. Geromanos SJ, Vissers JP, Silva JC, Dorschel CA, Li GZ, Gorenstein MV, Bateman RH, Langridge JI (2009) The detection, correlation, and comparison of peptide precursor and product ions from data independent LC-MS with data dependant LC-MS/MS. Proteomics 9:1683–1695
20. Chambery A, Vissers JP, Langridge JI, Lonardo E, Minchiotti G, Ruvo M, Parente A (2009) Qualitative and quantitative proteomic profiling of cripto(−/−) embryonic stem cells by means of accurate mass LC-MS analysis. J Proteome Res 8:1047–1058
21. Delahunty CM, Yates JR (2007) MudPIT: multidimensional protein identification technology. Biotechniques 43:563, 565, 567 passim.
22. Lo Turco EG, Souza GH, Garcia JS, Ferreira CR, Eberlin MN, Bertolla RP (2010) Effect of endometriosis on the protein expression pattern of follicular fluid from patients submitted to controlled ovarian hyperstimulation for in vitro fertilization. Hum Reprod 25:1755–1766
23. Ferreira CR, Lo Turco EG, Saraiva SA, Bertolla RP, Perecin F, Souza GHFM, Murgu M, Garcia JS, Cortezzi SS, Meirelles FV, Klitzke CF, Cabral EC, Miglino MA, Porciuncula PM, Leal CLV EB Jr, Martins DdS, Ambrósio CE, D'Alexandri F, Smith LC, Eberlin MN (2010) Proteomics, metabolomis and lipidomics in reproductive biotechnologies: the MS solutions. Acta Scientiae Veterinariae 38:s277–s289
24. Dominguez F, Gadea B, Esteban FJ, Horcajadas JA, Pellicer A, Simon C (2008) Comparative protein-profile analysis of implanted versus non-implanted human blastocysts. Hum Reprod 23:1993–2000
25. Kanka J (2003) Gene expression and chromatin structure in the pre-implantation embryo. Theriogenology 59:3–19
26. Hamatani T, Carter MG, Sharov AA, Ko MS (2004) Dynamics of global gene expression changes during mouse preimplantation development. Dev Cell 6:117–131
27. Misirlioglu M, Page GP, Sagirkaya H, Kaya A, Parrish JJ, First NL, Memili E (2006) Dynamics of global transcriptome in bovine matured oocytes and preimplantation embryos. Proc Natl Acad Sci U S A 103:18905–18910
28. Toyoda M, Kojima M, Takeuchi T (2000) Jumonji is a nuclear protein that participates in the negative regulation of cell growth. Biochem Biophys Res Commun 274:332–336
29. Takeuchi T, Watanabe Y, Takano-Shimizu T, Kondo S (2006) Roles of jumonji and jumonji family genes in chromatin regulation and development. Dev Dyn 235:2449–2459
30. Pasini D, Cloos PA, Walfridsson J, Olsson L, Bukowski JP, Johansen JV, Bak M, Tommerup N, Rappsilber J, Helin K (2010) JARID2 regulates binding of the Polycomb repressive complex 2 to target genes in ES cells. Nature 464:306–310
31. Modarressi MH, Cameron J, Taylor KE, Wolfe J (2001) Identification and characterisation of a novel gene, TSGA10, expressed in testis. Gene 262:249–255
32. Behnam B, Modarressi MH, Conti V, Taylor KE, Puliti A, Wolfe J (2006) Expression of Tsga10 sperm tail protein in embryogenesis and neural development: from cilium to cell division. Biochem Biophys Res Commun 344:1102–1110